Nanoscale

Accepted Manuscript

This article can be cited before page numbers have been issued, to do this please use: A. Catalán-Latorre, M. Pleguezuelos-Villa , I. Castangia, M. L. Manca, C. Caddeo, A. Nacher, O. Díez-Sales, J. E. Peris, R. Pons, E. Escribano, A. M. Fadda and M. Manconi, *Nanoscale*, 2017, DOI: 10.1039/C7NR05929A.

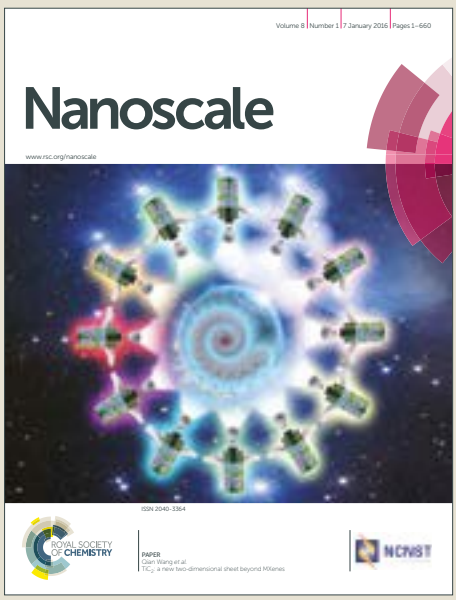

ROYAL SOCIETY OF CHEMISTRY

rsc.li/nanoscale

View Article Online
DOI: 10.1039/C7NR05929A

Nutriosomes: prebiotic delivery systems combining phospholipid, soluble dextrin and curcumin to counteract intestinal oxidative stress and inflammation

Ana Catalán-Latorre [1,6,+], Maria Pleguezuelos-Villa [2,3,+], Ines Castangia [1], Maria Letizia Manca [1,*], Carla Caddeo [1], Amparo Nácher [2,3], Octavio Díez-Sales [2,3], José Esteban Peris [2], Ramon Pons [4], Elvira Escribano-Ferrer [5], Anna Maria Fadda [1], Maria Manconi [1]

[1] Dept. of Scienze della Vita e dell'Ambiente, University of Cagliari, Cagliari, Italy

[2] Dept. of Pharmacy and Pharmaceutical Technology, University of Valencia, Valencia, Spain

[3] Institute of Molecular Recognition and Technological Development, Inter-Universitary Institute from Polytechnic University of Valencia and University of Valencia, Spain

[4] Dept. of Tecnologia Química i de Tensioactius, Institut de Química Avançada de Catalunya (IQAC-CSIC) 08034 Barcelona, Spain

[5] Biopharmaceutics and Pharmacokinetics Unit, Institute for Nanoscience and Nanotechnology, University of Barcelona, Barcelona, Spain

[6] Platform of Oncology, Hospital Quirón Torrevieja, Alicante, Spain

[+]These authors contributed equally to this work

* Corresponding author:

Maria Letizia Manca

Dept. Scienze della Vita e dell'Ambiente, University of Cagliari, via Ospedale 72, 09124 Cagliari, Italy

Tel.: +390706758582; fax: +390706758553

E-mail address: mlmanca@unica.it

View Article Online
DOI: 10.1039/C7NR05929A

ABSTRACT

Nutriosomes, new phospholipid nanovesicles specifically designed for intestinal protection were developed by simultaneously loading a water-soluble dextrine (Nutriose® FM06) and a natural antioxidant (curcumin). Nutriosomes were easily fabricated in a one-step, organic solvent-free procedure. The stability and the delivery performances of the vesicles were improved by adding hydroxypropylmetylcellulose. All the vesicles were small in size (mean diameter ~168 nm), negatively charged (zeta potential ~-38 mV, irrespective of their composition), self-assembled predominantly in unilamellar vesicles stabilized by the presence of Nutriose®, which was located in both the inter-lamellar and inter-vesicle medium, as confirmed by cryo-TEM and SAXS investigation. The dextrin acted also as a cryo-protector, avoiding vesicle collapse during the lyophilization process, and as a protector against high ionic strength and pH changes encountered in the gastrointestinal environment. Thanks to the antioxidant properties of curcumin, nutriosomes provided an optimal protective effect against hydrogen peroxide-induced oxidative stress in Caco-2 cells. Moreover, these innovative vesicles showed promising efficacy *in vivo*, as they improved the bioavailability and the biodistribution of both curcumin and dextrin upon oral administration, which acted synergically in reducing colonic damage chemically-induced in rats.

Keywords: phospholipid vesicles; curcumin; nutriose; intestinal inflammation; prebiotic activity.

View Article Online
DOI: 10.1039/C7NR05929A

1. INTRODUCTION

Starchs are abundant, low-cost, renewable and biodegradable molecules frequently used in food, papermaking, packaging industries, and textiles as well as in medicine, pharmacy and cosmetics. Their indigestible form is often used as a fiber supplement, and they are indispensable constituents of healthy diet, since their daily use promotes beneficial physiological effects by lowering cholesterol, triglycerides, and glucose levels [1,2]. Additionally, exposure to stress, alcohol or drugs diminishes the populations of microorganisms that naturally flourish in human intestine, and some fibers can exert a prebiotic action by nourishing and replenishing the healthy flora of the digestive tract [3]. The dietary use of prebiotics can prevent diarrhoea, intestinal irritation, ulcer, and colon cancer. Dextrins are low-molecular weight carbohydrates derived from dextrose and obtained from the hydrolysis of starch. The indigestible form of dextrin is often used as a fiber supplement. Nutriose® is an indigestible dextrin fiber (85%), sugar free, off-taste, water soluble, and stable at low pH. It possesses α1-2, α1-3 linkages that cannot be hydrolysed in the small intestine of mammals, but are fermented by intestinal bacteria [4]. Previous studies demonstrated that a daily dose of up to ~90 g of Nutriose® is well tolerated in man and provides beneficial effects on intestinal flora [5]. Moreover, its use in pharmaceutical formulations can offer protection against colitis, in synergy with a natural flavonoid [6].

Antioxidant flavonoids have been widely used as protective and curative agents in intestinal pathologies, and chronic inflammatory colon disorders [7–9]. Their loading in nanoparticulate systems plays an important role in maximizing their efficacy, thanks to enhanced bioavailability and targeted delivery [6,10].

In the present work, a soluble dextrin (Nutriose® FM06) and a potent natural antioxidant, curcumin, were combined with phospholipids to obtain promising oral delivery systems, named nutriosomes. The novelty and the advances of this study include the development of nutriosomes by a smart and green method: they self-assembled predominantly in unilamellar nanovesicles where the dextrin is solubilized in the aqueous compartment within the vesicles, as well as in the inter-vesicle medium,

View Article Online
DOI: 10.1039/C7NR05929A

thus playing a double role of payload and vesicle structuring agent. Moreover, the simultaneous nanoincorporation of prebiotic Nutriose® and antioxidant curcumin provide a converging efficacy on intestinal health. Nutriosomes were further modified by adding hydroxypropylmetylcellulose, which is expected to improve their stability [11]. Nutriosomes were deeply characterized, and their *in vitro* and *in vivo* performances were studied. In particular, the *in vitro* resistance of vesicles to pH and ionic strength was evaluated, along with their internalization by intestinal cells, and their protective effect against oxidative stress. Moreover, the chemical stability of curcumin and its release from the vesicle formulations were investigated. The *in vivo* biodistribution of vesicles after oral administration and the efficacy against chemically-induced colitis were also evaluated.

2. EXPERIMENTAL SECTION

Materials

Soy phosphatidylcholine (Phospholipon® 90G, P90G) was purchased from Lipoid GmbH (Ludwigshafen, Germany). Nutriose FM06®, a soluble dextrin from maize, was kindly provided by Roquette (Lestrem, France). Curcumin, hydroxypropylmetylcellulose (HPMC), 2,4,6-trinitrobenzenesulfonic acid (TNBS), and other reagents were purchased from Sigma-Aldrich (Milan, Italy). All the products and solvents were of analytical grade.

Sample preparation

To prepare nutriosomes, P90G (320 mg), curcumin (20 mg), Nutriose® (100 mg), hydroxypropylmetylcellulose (2 mg, when appropriate) were weighed in a glass flask, hydrated with 2 ml of bidistilled water and left swelling for 5 h. Then, the suspension was sonicated (2 sec on and 2 sec off, 30 cycles; 13 microns of probe amplitude) with a high intensity ultrasonic disintegrator (Soniprep 150, MSE Crowley, London, UK). Liposomes without Nutriose® were used as a reference. The exact sample composition is reported in Table 1. The samples were purified from non-incorporated curcumin by dialysis against water using Spectra/Por® membranes (12-14 kDa MW cut-off; Spectrum Laboratories Inc., DG Breda, The Netherlands).

View Article Online
DOI: 10.1039/C7NR05929A

Vesicle characterization

Vesicle formation and morphology were assessed by cryogenic transmission electron microscopy (cryo-TEM). A thin aqueous film was formed by placing a drop of each sample on a glow-discharged holey carbon grid and then blotting it with filter paper. The resulting thin films were vitrified by plunging the grid (kept at 100% humidity and room temperature) into ethane maintained at its melting point, using a Vitrobot (FEI Company, Eindhoven, The Netherlands). The vitreous films were transferred to a Tecnai F20 TEM (FEI Company) using a Gatan cryotransfer (Gatan, Pleasanton, CA), and the samples were observed in a low-dose mode. Images were acquired at 200 kV at a temperature between -170/-175 °C by using low-dose imaging conditions not exceeding 20 $e^{-}/Å^{2}$, with a CCD Eagle camera (FEI Company).

The intensity-weighted mean diameter and polydispersity index (PI; a dimensionless measure of the broadness of the size distribution) were determined by Photon Correlation Spectroscopy using a Zetasizer nano-ZS (Malvern Instruments, Worcestershire, UK), which analyzes the fluctuations in intensity of the light backscattered by particles in dispersion. Zeta potential was estimated using the Zetasizer nano-ZS by means of the M3-PALS (Mixed Mode Measurement-Phase Analysis Light Scattering) technique, which measures the particle electrophoretic mobility.

Curcumin content was quantified after disruption of the vesicles with methanol (1:1000), by using a HPLC chromatograph (Thermo Scientific, Madrid, Spain) equipped with a C18 Novapak column (Waters, Madrid, Spain). The mobile phase consisted of a mixture of acetonitrile/water/acetic acid (50:49:1), delivered at a flow rate of 1 ml/min, and detection was performed at 425 nm. The entrapment efficiency (EE%) was calculated and expressed as the percentage of curcumin post-dialysis *vs.* pre-dialysis.

Vesicle stability

The vesicle dispersions were stored at 25 °C for 90 days, and their mean diameter, polydispersity index and zeta potential were measured at different time points. In parallel, the dispersions were

View Article Online
DOI: 10.1039/C7NR05929A

freeze-dried, stored at 25 °C in air or under vacuum, and rehydrated at scheduled time periods to measure the mean diameter, polydispersity index and zeta potential.

Vesicle behaviour at gastrointestinal pHs

The vesicles (1 ml) were diluted with 9 ml of an acidic solution (pH 2) or a neutral solution (pH 7) containing sodium chloride (0.3 M), transferred into the basket of a dissolution rotating apparatus (US Pharmacopeia), thermostated at ~37°C and maintained for 2 h at pH 2, or for 6 h at pH 7. The mean diameter, polydispersity index and zeta potential of the vesicles were measured immediately after the dilution and at the end of the experiments.

Small-Angle X-ray Scattering (SAXS)

SAXS measurements were performed at the BL11-NCD (Non-Crystalline Diffraction) beamline at ALBA synchrotron facility (Cerdanyola del Vallès, Barcelona, Spain). The X-ray beam had a flux of 10^{12} photons/sec, with an energy of 10 keV and wavelength of 0.124 nm. The usable q range was 0.09-4.77 nm^{-1}. The samples were loaded in a flow through glass capillary mounted on an Anton Paar (Graz, Austria) KPR Peltier sample stage, which kept the temperature at 25 ºC. The ensemble was fixed to a motorized sample-stage, which allowed the sample to be aligned and oriented in the beam. Bidimensional X-ray scattering patterns were acquired using an ADSC Quantum 210r CCD detector. Exposure time per frame was 5 sec. The images were radially averaged and summed. Two series of diffraction patterns were obtained from the same capillary with a separation of 500 μm to check for reproducibility and possible radiation damage (which was not detected throughout the experiments). SAXS patterns were analyzed using a home-made fitting procedure based on a Gaussian description of the bilayers. Since symmetric bilayers did not give an accurate description of the spectra, the possibility of having different electronic density in the polar head region of one and the other side of the bilayer was introduced [12]. The fitting model previously described by Caddeo et al. [12], was employed with a slight modification of the equation used to describe the polar

View Article Online
DOI: 10.1039/C7NR05929A

heads represented by a symmetric Gaussian function, using $\Delta\rho_{h1}$ and $\Delta\rho_{h2}$ instead of an additional Gaussian (Eq. 1):

$$G_{h1}(z) = \frac{1}{\sqrt{2\pi}}\Delta\rho_{h1}\exp\left(-\frac{(z-z_{h1})^2}{\sigma_{h1}^2}\right) + \frac{1}{\sqrt{2\pi}}\Delta\rho_{h2}\exp\left(-\frac{(z+z_{h1})^2}{\sigma_{h1}^2}\right)$$

***In vitro* bioactivity of curcumin formulations against oxidative stress**

Caco-2 cells were grown as monolayer in 75 cm^2 flasks, at 37 °C in humidified atmosphere of 5% CO_2 in air. Dulbecco's Modified Eagle Medium high glucose, containing L-glutamine, supplemented with 10% foetal bovine serum, 1% penicillin/streptomycin and 1% fungizone, was used as growth medium. Cells were seeded into 96-well plates at a density of 7.5×10^3 cells/well. After 24 h of incubation, cells were exposed to hydrogen peroxide (1:30000 dilution) for 4 h, in the presence or absence of curcumin in aqueous dispersion or loaded in vesicles (final concentration of curcumin 20 μg/ml). Cells treated with hydrogen peroxide-only were used as a positive control. After 4 h of incubation, the cells were washed with fresh medium, and their viability was determined by the MTT [3(4,5-dimethylthiazolyl-2)-2, 5-diphenyltetrazolium bromide] colorimetric assay, by adding 100 μl of MTT reagent (0.5 mg/ml in PBS) to each well. After 3 h, the formed formazan crystals were dissolved in dimethyl sulfoxide, and the concentration was spectrophotometrically quantified at 570 nm with a microplate reader (Synergy 4, Reader BioTek Instruments, AHSI S.p.A, Bernareggio, Italy). The results are reported as the percentage of untreated cells (100% viability).

***In vitro* curcumin stability and release**

The stability of curcumin loaded in vesicles was assessed by monitoring the chromatographic profile and the concentration of the polyphenol over 8 h of incubation in cell medium under constant stirring at 37 °C, by HPLC (see Vesicle characterization section).

The release of curcumin from the vesicles was measured by diluting the formulations (2 ml) with cell medium (2 ml), and keeping the dispersions under stirring for 8 h at 37 °C. At regular time intervals (2, 4, 6 and 8 h), samples were centrifuged at 10000 rpm for 5 min at 0 °C. After

View Article Online
DOI: 10.1039/C7NR05929A

centrifugation, the formation of three strata was observed: the superior one was yellow transparent and contained the smaller vesicles, the intermediate one was gel-like and yellowish and contained the larger vesicles, and the inferior one was intensely coloured in yellow/orange and contained free curcumin. The two vesicle strata were recovered and the initial volume (4 ml) was restored with fresh medium to continue the release study, while the pellet was solubilized in methanol to quantify curcumin by HPLC.

***In vitro* cell uptake of vesicles**

Caco-2 cells were grown as monolayer in poly-L-Lysine coated 8-well μ-slide (Ibidi GmbH, Martinsried, Germany) and incubated with the vesicles labelled with 1,2-dioleoyl-sn-glycero-3-phosphoethanolamine-N-(lissamine rhodamine B sulfonyl (Rho-PE; Avanti Polar Lipids, Alabama), and 5(6)-carboxyfluorescein (CF, Sigma-Aldrich, Milan, Italy). The uptake of the vesicles was investigated in living cells, at 1, 2 and 4 h, by confocal laser scanning microscopy (CLSM) using a FluoView FV1000 confocal microscope (Olympus, Barcelona, Spain). Pictures were taken in z-stacks using a 60× objective.

***In vivo* studies**

In vivo studies adhered to the principles of laboratory animal care and use, and were performed in accordance with the European Union regulations for the handling and use of laboratory animals and the protocols were approved by the Institutional Animal Care and Use Committee of the University of Valencia (code 2016/VSC/PEA/00159 type 2). Male Wistar rats, aged 8-12 weeks and weighing 230-250 g, were housed in air-conditioned rooms at 22±3°C, 55±5% humidity, 12 h light/dark cycles, with free access to water and chow.

Intestinal biodistribution of hydrophilic macromolecules

Phycocyanin, a macromolecular, hydrophilic, fluorescent marker, was used to label the vesicles and possibly predict the distribution of Nutriose®. The labelled vesicles or the phycocyanin solution (2 ml) were intragastrically administered to healthy rats by gavage (n=4 per group). At 3, 5 and 7 h,

View Article Online
DOI: 10.1039/C7NR05929A

rats were sacrificed, the intestines removed, slightly stretched and carefully spread on a dissecting board, and observed by using the In-Vivo FX PRO Imaging System (Bruker BioSpin, USA). Phycocyanin biodistribution was observed (excitation at 640 nm and emission at 680 nm), while curcumin fluorescence overlapped with the spectrum of the intestinal lumen content.

Intestinal biodistribution of curcumin

Curcumin dispersion or curcumin loaded vesicles (2 ml) were intragastrically administered to healthy rats by gavage (n=4 per group). After 3 h, the rats were sacrificed, and liver, kidneys and intestines were excised. The intestines were emptied and divided in segments: duodenum, jejunum, cecum and colon, slightly stretched and carefully spread on a dissecting board. Liver, kidneys, and intestine specimens were soaked in acetonitrile:water (70:30), homogenized and centrifuged at 12500 rpm for 10 min. The amount of curcumin was quantified by HPLC (see Vesicle characterization section). Results were expressed as the ratio of the amount of curcumin in the harvested organ *vs.* the amount of curcumin administered.

Pharmacokinetics of curcumin

Twenty-four hours before curcumin administration, animals were subjected to jugular vein cannulation, and after surgery, they were allowed to recover from the anesthesia. 3 ml of curcumin dispersion (10 and 20 mg/ml) or curcumin loaded vesicles (10 mg/ml) were intragastrically administered to healthy rats by gavage (n=5 per group). After administration, blood samples (0.2 ml) were withdrawn into heparinized syringes at scheduled time points, up to 8 h. Each blood sample was deproteinized with acetonitrile and centrifuged at 3000 rpm for 5 min, and the plasma was stored at -20ºC until assayed for curcumin content by HPLC. The chromatographic analyses were performed in a Perkin Elmer® HPLC Series 200 equipped with a binary pump, an auto-sample and a fluorescence detector. Identification and quantification of curcumin were performed in a Teknokroma® Brisa "LC2" C18 column (5.0 μm, 150 × 4.6 mm). Curcumin was eluted isocratically at a flow rate of 1 ml/min using 20 mM acetate buffer pH 3.0 and methanol (40:60, v/v) as a mobile

View Article Online
DOI: 10.1039/C7NR05929A

phase, and 50 µl for the injection volume. Excitation and emission wavelengths of elute fluorescence were optimized for measurement at 420 and 530 nm, respectively.

The pharmacokinetic parameters were calculate using a non-compartmental analysis by Phoenix WinNonlin®. The maximum observed plasma concentration (C_{max}) and the time taken to reach it (t_{max}) were obtained from the curve plotting curcumin concentration *vs.* time. The area under each drug concentration time curve (AUC, ng/ml h) to the last data point was calculated by the linear trapezoidal rule and extrapolated to time infinity by the addition of C_{Last}/Ke, where C_{Last} is the concentration of the last measured plasma sample.

Efficacy of curcumin against colitis

Chronic inflammation in rat colon was chemically induced as previously described [6,13], with slight modifications. Rats (n=4 per group) were anesthetized with isoflurane, and TNBS (0.13 M) dissolved in ethanol/water (50:50) was instilled (0.5 ml) into the colon lumen (day 0). Healthy animals were the negative control; animals with TNBS-induced colitis treated with saline were the positive control; the other groups consisted of animals with colitis receiving curcumin dispersion or curcumin liposomes, nutriosomes or HPMC-nutriosomes (2 ml) by oral gavage daily for 3 days, when inflammation was most intense (days 3, 4 and 5 after TNBS rectal administration).

On day 9, the rats were euthanized with an overdose of sodium pentobarbital (Dolethal®, Vetoquinol, UK), the abdomen was cut open, and the distal colon was removed. The extent and severity of colitis was evaluated by visual inspection of the excised colon, along with the measurement of myeloperoxidase activity (MPO). MPO was used as an index of inflammation and was measured according to an established method [6,13]. Briefly, each colon specimen was soaked in 750 µl of hexadecyltrimethylammonium bromide buffer (0.5% in 80 mM phosphate buffer pH 5.4) and homogenized. The homogenate was centrifuged (Heraeus Fresco 17 Centrifuge, Thermo Electron Corporation, Spain) at -1°C and 1000 rpm for 15 min. The supernatant was incubated with

View Article Online
DOI: 10.1039/C7NR05929A

hydrogen peroxide and tetramethylbenzidine. The reaction was stopped with 2 N H_2SO_4, and the absorbance was measured spectrophotometrically at 450 nm.

Statistical analysis of data

Results are expressed as the mean±standard deviation. Analysis of variance (ANOVA test) was performed to assess the differences among groups using the IBM SPSS statistics 20.0 for Windows. Post hoc testing (p=0.05) of multiple comparisons was performed by the Scheffe or Dunnet tests.

3. RESULTS

Vesicle characterization

Nutriosomes, HPMC-nutriosomes and liposomes were easily fabricated in a one-step procedure, without the use of organic solvents or energetic and dissipative procedures, by keeping the phospholipid and the other components in water, and by sonicating the dispersion to form lamellar vesicles and adjust their size and lamellarity. The sample composition is reported in Table 1.

Table 1. Composition of curcumin loaded liposomes, nutriosomes and HPMC-nutriosomes.

	P90G (mg/ml)	Curcumin (mg/ml)	Nutriose (mg/ml)	HPMC (mg/ml)
Liposomes	160	10	0	0
Nutriosomes	160	10	50	0
HPMC-nutriosomes	160	10	50	1

The actual formation of the vesicles and their morphology were confirmed by cryo-TEM observation. The images of liposomes displayed spherical and mostly unilamellar vesicles, with a few multilamellar vesicles (Figure 1A). Nutriosomes were spherical in shape, and both multilamellar, multicompartment structures and unilamellar vesicles were observed (Figure 1B). HPMC-nutriosomes were basically spherical and unilamellar (Figure 1C).

View Article Online
DOI: 10.1039/C7NR05929A

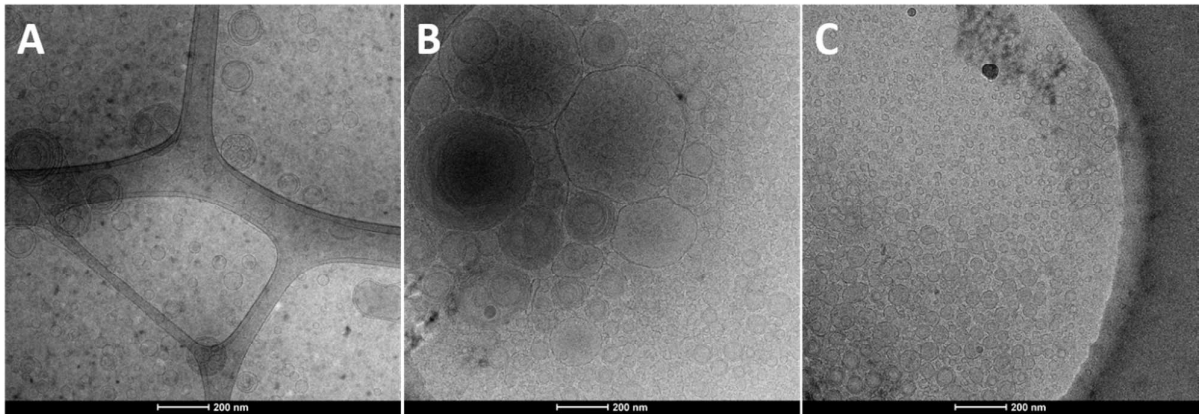

Figure 1. Representative cryo-TEM images of curcumin loaded liposomes (A), nutriosomes (B) and HPMC-nutriosomes (C).

The mean diameter of empty liposomes was ~107 nm, and the addition of curcumin led to a significant increase in size up to ~181 nm ($p<0.01$) and zeta potential from -12 to -37 mV ($p<0.01$), which indicate a localization of curcumin not only within the bilayer, but also onto the bilayer surface (Table 2) [14,15].

Table 2. Mean diameter (MD), polydispersity index (PI), zeta potential (ZP) and entrapment efficiency (EE) of empty and curcumin loaded liposomes, nutriosomes and HPMC-nutriosomes. Mean values (n=6) ± standard deviation are reported. Different symbols (#, *) indicate statistically different values.

	MD (nm)	**PI**	**ZP (mV)**	**EE (%)**
Empty liposomes	107±8	0.35	-12±4	
Empty nutriosomes	127±7	0.24	-13±3	
Empty HPMC-nutriosomes	135±6	0.31	-14±6	
Curcumin liposomes	181±7	0.33	-37±4	#73±6
Curcumin nutriosomes	183±8	0.35	-39±2	*88±7
Curcumin HPMC-nutriosomes	153±8	0.34	-36±7	*91±6

View Article Online
DOI: 10.1039/C7NR05929A

The addition of Nutriose® led to a small increase of the mean diameter of empty nutriosomes in comparison with empty liposomes (from ~107 to ~127 nm, $p<0.05$), while in curcumin loaded nutriosomes the effect of the dextrin was mitigated by the presence of the polyphenol, as liposomes and nutriosomes showed the same mean diameter and zeta potential (~182 nm and ~-38 mV, $p>0.05$ between the two samples). The further addition of HPMC led to a slight increase in size for empty nutriosomes, while a decrease was observed upon incorporation of curcumin (~153 nm, $p<0.05$ *vs.* liposomes and nutriosomes).

The stability of the vesicle dispersions was evaluated during storage at 25°C. After 60 days, the mean diameter of all the samples significantly increased (data not shown). As an alternative, the dispersions were freeze-dried and kept at 25°C in air or under vacuum. The samples were rehydrated every 30 days up to 180 days, and the size, polydispersity index and zeta potential were measured (Figure 2).

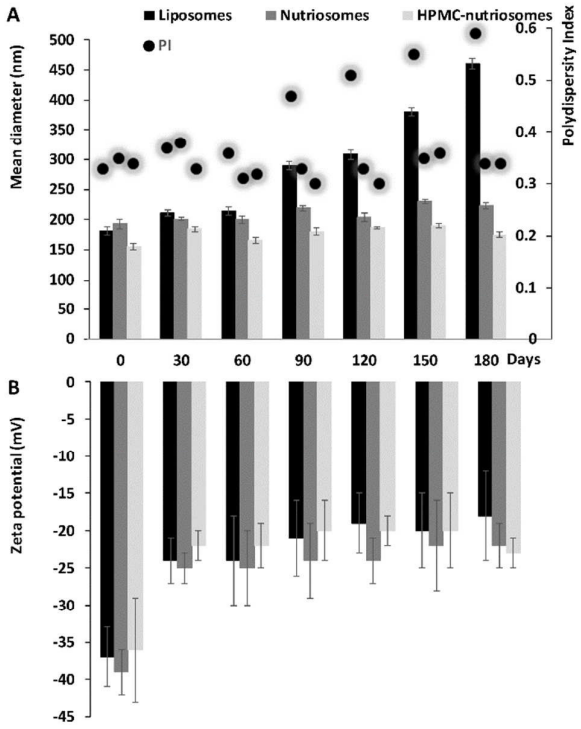

View Article Online
DOI: 10.1039/C7NR05929A

Figure 2. Mean diameter, polydispersity index (PI) and zeta potential of curcumin loaded liposomes, nutriosomes and HPMC-nutriosomes lyophilized, kept under vacuum for 180 days, and rehydrated at different time periods. Bars represent standard deviations (n=3).

The size of liposomes remained almost constant during the first 60 days, then the mean diameter and polydipersity index increased up to ~450 nm and 0.6, respectively. On the contrary, the parameters of both nutriosomes and HPMC-nutriosomes remained constant over the whole storage period, indicating a positive effect of Nutriose® on the vesicle re-formation, probably because the soluble dextrin acted as a cryo-protector avoiding structural collapse of the vesicles during the dehydration process.

The resistance of the vesicles to pH variations and ionic strength was evaluated by incubating the formulations with appropriate solutions (pH 2 or 7 and 0.3 M NaCl), and monitoring the vesicle size, polydispersity index and zeta potential (Table 3) [6].

Table 3. Mean diameter (MD), polydispersity index (PI), zeta potential (ZP) and entrapment efficiency (EE) of liposomes, nutriosomes and HPMC-nutriosomes diluted and incubated with acidic solution (pH 2) for 2 h or with neutral solution (pH 7) for 6 h, both containing sodium chloride (0.3 M), at 37°C. The measurements were carried out immediately after the dilution (t_{0h}) and after 2 h at pH 2 (t_{2h}) and 6 h at pH 7 (t_{6h}). Mean values ± standard deviation are reported.

	pH	Time	MD (nm)	PI	ZP (mV)	EE (%)
Liposomes	2	t_{0h}	205±40	0.41	13±3	
		t_{2h}	557±20	0.58	11±2	79±6
Nutriosomes	2	t_{0h}	174±15	0.37	13±4	
		t_{2h}	394±49	0.50	8±5	93±10
HPMC-nutriosomes	2	t_{0h}	199±19	0.40	10±4	
		t_{2h}	224±42	0.49	9±5	89±9
Liposomes	7	t_{0h}	181±20	0.42	0±2	
		t_{6h}	162±5	0.39	-1±2	33±12

View Article Online
DOI: 10.1039/C7NR05929A

Nutriosomes	7	t_{0h}	170±7	0.47	0±2	
		t_{6h}	166±49	0.41	-4±3	49±5
HPMC-nutriosomes	7	t_{0h}	134±21	0.48	-2±5	
		t_{6h}	204±8	0.49	-1±2	56±7

After 2 h at pH 2, the size of liposomes increased up to 557 nm and the polydispersity index up to 0.58, which indicats a partial loss of their structure. On the contrary, the size of nutriosomes was less affected by the acidic pH (394 nm), and even less in the case of HPMC-nutriosomes (224 nm). Under these conditions, the zeta potential of the samples turned to positive values. After 6 h at pH 7, both liposomes and nutriosomes did not undergo marked alterations, while HPMC-nutriosomes increased in size, presumably due to swelling, which follows polymer hydration leading to relaxation of polymer chains and their entanglement to form a viscous gel layer around the vesicles.

SAXS analysis

Empty liposomes showed the typical spectra of multilamellar vesicles (Figure 3A), with a large number of unilamellar (i.e., uncorrelated) structures (20% correlation; Table 4), while curcumin loaded liposomes (phospholipid:curcumin molar ratio 8.6:1) were predominantly unilamellar, with a small population (6%; Table 4) of multilamellar (i.e., correlated) vesicles (Figure 3A).

The multilamellar liposomes, from both spectra, showed similar repetition distance (d, 6.21 and 6.28 nm for empty and curcumin loaded liposomes, respectively; Table 4). Because of the high preponderance of unilamellar vesicles, the parameters associated with the structure (Caillé parameter η, and number of correlated and uncorrelated lamellae N and N_{unc}) have high uncertainty. The main differences in the bilayer structure of empty and curcumin loaded liposomes refer to the width of the head group and methylene gaussians (σ_h and σ_c, respectively; Table 4), which are smaller for curcumin loaded liposomes, as can also be observed in the electron density plots showing more pronounced polar head and methylene gaussians (Figure 3B). This is in contrast with the observations of Hung et al. [16] that observed an increase of both σ_h and σ_C when curcumin was added to dioleoylglycerophosphocholine liposomes. Moreover, Hung et al. detected a reduction in

View Article Online
DOI: 10.1039/C7NR05929A

the phosphate peak-to-phosphate peak distance (equivalent to 2 Z_h) of about 0.1 nm for curcumin/lipid molar ratios above 0.02, while we observed a reduction of 0.03 nm at the present curcumin/lipid molar ratio of 0.13. However, it has to be noted that Hung et al.'s experiments were conducted below complete hydration.

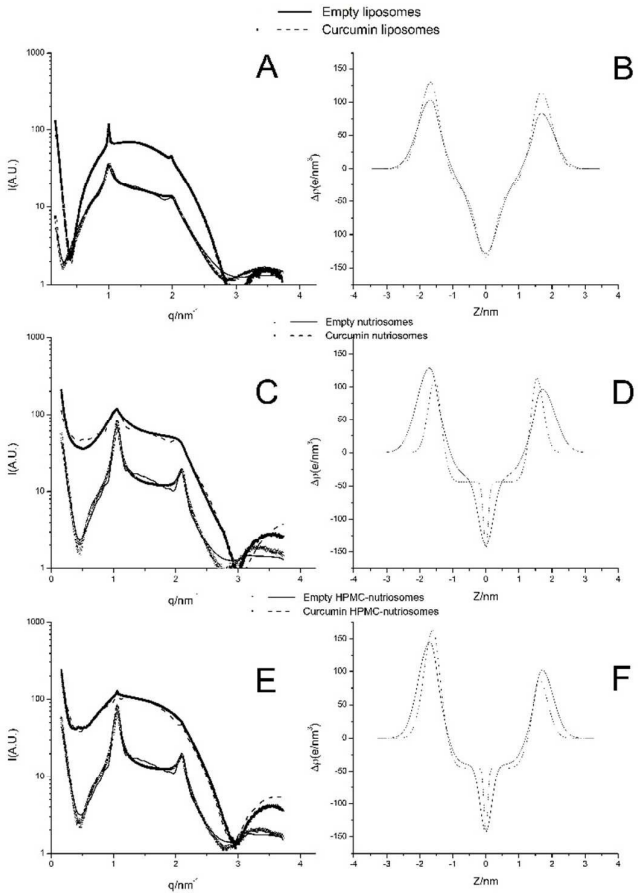

Figure 3. Experimental SAXS intensity (symbols) and fitted model (lines) are shown in the left panel, electron density profiles in the right panel for empty and curcumin loaded liposomes (A-B), nutriosomes (C-D), and HPMC-nutriosomes (E-F).

View Article Online
DOI: 10.1039/C7NR05929A

The electron density of the polar head ($\Delta\rho_h$; Table 4) increased when curcumin was loaded, which might be a consequence of curcumin replacing some of the water molecules that hydrate the polar heads.

The scattering profiles of empty and curcumin loaded nutriosomes were the result of the subtraction of Nutriose® (50 mg/ml) spectrum (Figure 3C). The profile of empty nutriosomes showed the typical peaks of multilamellar vesicles (corresponding to 42% of the sample; Table 4). Nutriose® seems to interact weakly with the bilayer, as demonstrated by the similar spectra of empty liposomes and nutriosomes. This can be explained by the fact that water-soluble Nutriose® is supposedly localized in the aqueous compartments of the vesicles (internal core, interlamellar space, and intervesicle medium). However, the dextrin seems to affect the arrangement of the vesicles, as it increased the lamellarity (from 20 to 42% of multilamellar structures; Table 4) and rigidity observed as a significant reduction of Caillé parameter (η; Table 4) when comparing the results of nutriosomes and liposomes. These effects can be due to the ability of Nutriose® to reduce the interlamellar repulsion due to its solubilization in the aqueous layers where solvent dielectric constant is decreased as a result of the increased number of ionized groups on the interfacial bilayer regions [17,18].

Table 4. Fitting derived parameters obtained from SAXS analyses at 25 °C of empty and curcumin loaded liposomes, nutriosomes and HPMC-nutriosomes. Mean values ± standard deviation are reported.

	Empty liposomes	**Empty nutriosomes**	**Empty HPMC-nutriosomes**	**Curcumin liposomes**	**Curcumin nutriosomes**	**Curcumin HPMC-nutriosomes**
d (nm)	6.21±0.05	5.97±0.05	5.97±0.05	6.28±0.05	6.10±0.05	5.98±0.05
η	0.10±0.04	0.06±0.01	0.07±0.01	0.12±0.05	0.04±0.04	0.05±0.01
N	5.9±2	7.9±1	8.0±1	54±2	3.9±1	15±4
σ_h (nm)	0.39±0.05	0.39±0.05	0.35±0.05	0.33±0.05	0.42±0.02	0.15±0.05
$\Delta_{\rho h1}$ (e/nm^3)	83±5	97±5	102±5	115±5	52±5	89±5

View Article Online
DOI: 10.1039/C7NR05929A

$\Delta_{\rho h2}$ (e/nm^3)	103±5	129±5	146±5	129±5	53±5	168±5
Z_h (nm)	1.67±0.05	1.70±0.05	1.69±0.05	1.66±0.05	1.63±0.05	1.60±0.05
σ_c (nm)	0.35±0.10	0.22±0.10	0.17±0.10	0.29±0.10	0.07±0.10	0.05±0.10
N_{unc}	24±5	11±5	10±5	800±100	5.9±2	650±1000
% correlation	20	42	43	6	29	2

d, repetition distance; η, Caillé parameter; N, number of correlated lamellae; σ_h, polar head Gaussian width with electron density difference to the media, $\Delta_{\rho h1}$ and $\Delta_{\rho h2}$, for each bilayer leaflet; Z_h, position of the polar head Gaussian with respect to the bilayer center; σ_c, methylene groups Gaussian width at the center of the bilayer; N_{unc}, number of uncorrelated lamellae.

A reduction of the lamellar spacing was also observed (d, from 6.21 to 5.97 nm; Table 4), which may be caused by an increase in rigidity of the bilayers. On the other hand, the presence of curcumin reduced the intensity of the peaks, and the bands corresponding to unilamellar vesicle predominate. When comparing the electron density profiles of empty and curcumin loaded nutriosomes, the main finding is the thinning of the bilayer (i.e., decrease in thickness) when curcumin was loaded, due to the dehydration of the polar heads (Figure 3D; σ_H, Table 4). At the same time, the hydrophobic part (Figure 3C; σ_C, Table 4) of the phospholipid became more ordered, and the dip due to the methylene groups became more distinct, which is probably a consequence of the partial dehydration of the polar heads.

In Figure 3E, the spectra of empty and curcumin loaded HPMC-nutriosomes are reported. As can be deduced by comparing the spectra of HPMC-nutriosomes and nutriosomes, the effect of HPMC on the bilayer structure and ordering is minimal. Again, curcumin reduced notably the number of multilamellar vesicles (from 43 to 2%; Table 4), as only a small signal corresponding to multilamellar structures was still visible. The effect of curcumin was very similar to that observed in curcumin loaded liposomes, which showed a spectrum typical of an entirely unilamellar vesicle system, with a small population (6% and 2% for curcumin liposomes and HPMC-nutriosomes, respectively; Table 4) of significantly multilayered vesicles. This effect can be deduced from the

View Article Online
DOI: 10.1039/C7NR05929A

comparison of the number of correlated bilayers and uncorrelated bilayers (N and N_{unc}, respectively; Table 4).

While the asymmetry of the bilayer (as quantified by the difference between $\Delta\rho_{h1}$ and $\Delta\rho_{h2}$) is only marginally affected by the presence of Nutriose®, it seems clear that the presence of HPMC has a strong effect, increasing the electron density difference (Figure 3F). We should remark that a similar effect on the fitting could be obtained by letting the headgroup position to differ, instead of the electron density, because both have a strong cross-correlation and the fits of the HPMC were not optimal.

Summarizing, we can say that the effect of curcumin is dramatic on the SAXS profiles of all the vesicle systems studied, which is not on the bilayer thickness and electron density distribution, but on the lamellarity. At present, the reason behind the strong increase in the presence of uncorrelated lamellae (i.e., unilamellar structures) is not clear. The overall effect of curcumin on the bilayer is an increase in rigidity (decrease of Caillé parameter η) and a reduction of the width of the polar heads (σ_h). On the other hand, the presence of Nutriose® and HPMC increase the dissymmetry of the bilayer, which suggests that they partition preferably to one of the leaflet. Since the model does not distinguish between the inner and the outer leaflet, we cannot say whether Nutriose® and HPMC are localized/adsorbed in the concave or convex leaflet.

***In vitro* bioactivity of curcumin formulations against oxidative stress**

The ability of curcumin loaded vesicles to neutralize free radicals and protect Caco-2 cells from oxidative stress caused by hydrogen peroxide was demonstrated, as compared to the effect of curcumin dispersion at the same concentration (Figure 4).

View Article Online
DOI: 10.1039/C7NR05929A

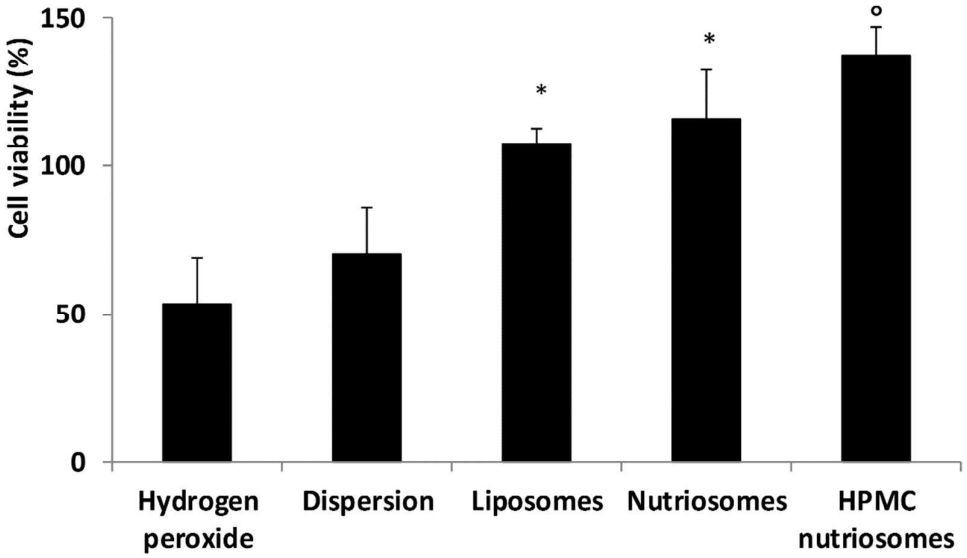

Figure 4. Viability of Caco-2 cells exposed to hydrogen peroxide alone or simultaneously treated with curcumin aqueous dispersion or curcumin loaded liposomes, nutriosomes and HPMC-nutriosomes. Data are reported as mean values ± standard deviation (error bars) of cell viability expressed as the percentage of the negative control (100% viability). *,° different symbols indicate statistically different values ($p<0.05$).

After hydrogen peroxide exposure, cell viability was halved (~50%). It increased slightly when the curcumin dispersion was applied (~70%, $p>0.05$), to a greater extent when using curcumin loaded liposomes and nutriosomes (~110%, $p<0.05$ between liposomes and nutriosomes, and $p<0.01$ *vs.* hydrogen peroxide-exposed cells), and even more when using HPMC-nutriosomes (~137%, $p<0.01$ *vs*. all the samples). The results highlighted the important role played by the phospholipid vesicles in enhancing the activity of curcumin, and a further improvement provided by HPMC.

***In vitro* curcumin stability and release**

The chromatographic profiles of curcumin did not show significant variations after incubation in cell medium for 8 h, and the concentration of curcumin did not decrease. This demonstrates that no degradation occurred, thus proving the stability of the polyphenol under the experimental conditions tested (Figure 5 A and B) [19].

View Article Online
DOI: 10.1039/C7NR05929A

The amount of curcumin released from liposomes reached a maximum at 2 h (~80%), and remained constant up to 8 h. On the contrary, the release of curcumin from nutriosomes and HPMC-nutriosomes was lower at 2 and 4 h (~32 and 58%, respectively), and reached 68% at 8 h (Figure 5 c).

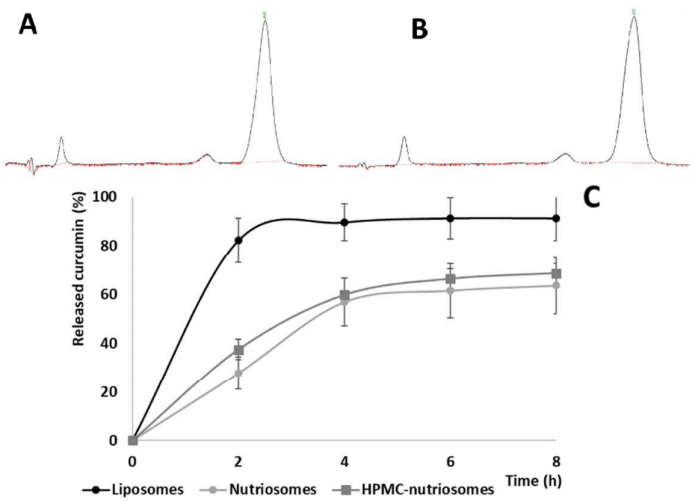

Figure 5. Representative chromatograms of curcumin before (A) and after 8 h of incubation (B) of curcumin liposomes, nutriosomes and HPMC-nutriosomes in cell medium.

Release profiles of curcumin from liposomes, nutriosomes and HPMC-nutriosomes (C) over 8 h in cell medium.

In vitro cell uptake

The uptake of liposomes, nutriosomes and HPMC-nutriosomes by Caco-2 cells was evaluated after 1, 2 and 4 h of incubation with the vesicles labelled with Rho-PE, as a lipid marker (red fluorescence), and CF, as a hydrophilic marker (green fluorescence) (Figure 6). The images of cells incubated with liposomes, at 1, 2 and 4 h disclosed a non-time dependent accumulation of Rho-PE in the perinuclear area, while no localisation of CF within the cells was observed, as it was confined to the external medium. This may indicate that a rupture of liposomes occurred during the internalization process. The images of the cells treated with labelled nutriosomes showed a different

View Article Online
DOI: 10.1039/C7NR05929A

behaviour: Rho-PE was localized in the perinuclear area, CF was mainly accumulated in the cytoplasm, and a yellow fluorescence was also observed in the peripheral area of the cytoplasm, which indicates the co-localization of the two probes presumably internalized in intact vesicles. The cells incubated with HPMC-nutriosomes showed an even more evident co-localization of the probes. The yellow fluorescence was similar to that observed for nutriosomes after 1 h of incubation, while it was more intense at 2 and 4 h, which indicates a massive internalization of vesicles and aggregation in the peripheral area of the cytoplasm. The increased uptake of HPMC-nutriosomes is probably related to the presence of the polymer, which may favour the interaction between cells and vesicles.

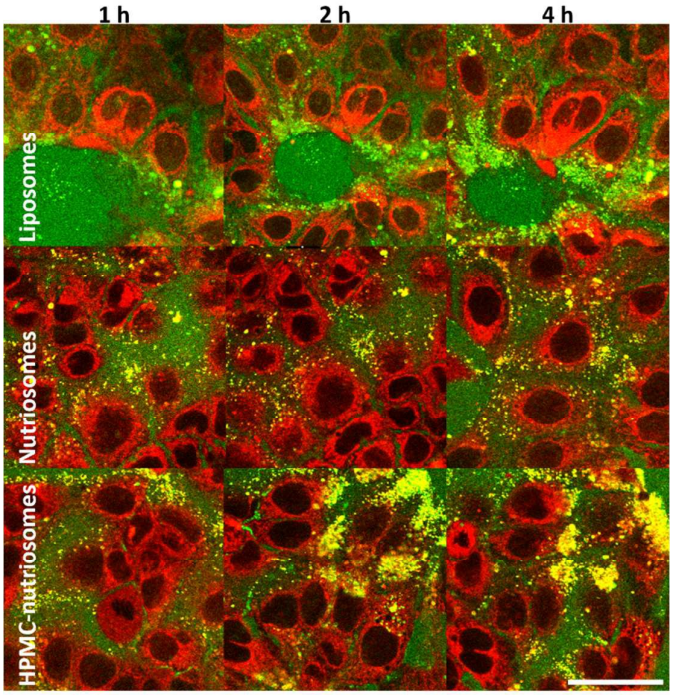

Figure 6. CLSM images of Caco-2 cells exposed to liposomes, nutriosomes and HPMC-nutriosomes labelled with Rho-PE (red) and CF (green) for 1, 2 and 4 h. The bar corresponds to 50 μm.

***In vivo* biodistribution of hydrophilic macromolecules in the gastrointestinal tract**

View Article Online
DOI: 10.1039/C7NR05929A

To evaluate the gastrointestinal transit of the formulations and to establish their ability to facilitate dextrin and curcumin delivery *in vivo*, the vesicles were labelled with phycocyanin, which is a water-soluble, fluorescent macromolecule [20]. The labelled vesicles loading curcumin were administered to healthy rats, and their biodistribution in the gastrointestinal tract was monitored as a function of time by using the In Vivo FX PRO Imaging System, which allowed the precise localization of the markers. An aqueous dispersion of phycocyanin and curcumin was also administered and used as a reference. The fluorescence of phycocyanin was visualized in blue, while the fluorescence of curcumin overlapped with the spectrum of the intestinal lumen content (Figure 7). When the phycocyanin solution was administered, the fluorescence decreased over time: after 3-5 h, the fluorescence was moderate and restricted to the final part of the intestine, mostly jejunum and slightly in the cecum and colon, while it disappeared after 7 h. Liposomes provided a more widespread and persistent fluorescence in comparison with the solution: after 3-5 h, the signal was more evident in duodenum and jejunum, and after 7 h, a weak signal was visible also in cecum and colon.

View Article Online
DOI: 10.1039/C7NR05929A

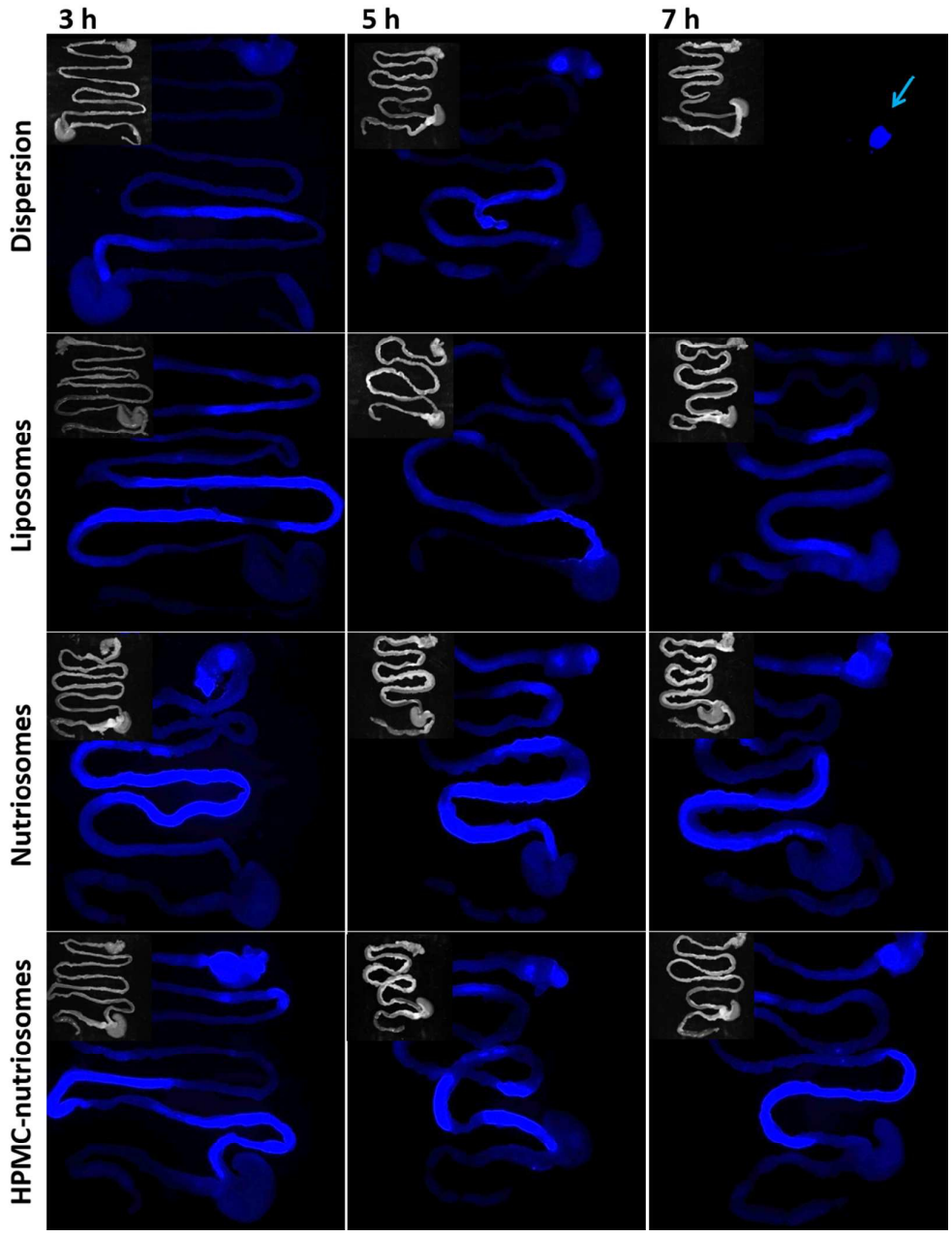

Figure 7. Fluorescence images of the gastrointestinal tract excised from healthy rats treated with a dispersion of phycocyanin and curcumin or phycocyanin-labelled curcumin-loaded liposomes, nutriosomes and HPMC-nutriosomes.

After nutriosome administration, the most intense fluorescence was observed: after 3 h, it was diffused in the stomach, duodenum and upper part of jejunum; after 5 h, it shifted in the whole jejunum and slightly in the cecum; after 7 h, it was detected in the final part of jejunum and slightly

View Article Online
DOI: 10.1039/C7NR05929A

in cecum and colon. After HPMC-nutriosome administration, the florescence distribution was similar to that observed for nutriosomes, but less intense and extensive. Hence, all the vesicles enhanced the fluorescence biodistribution and intensity with respect to that provided by the solution, and especially nutriosomes were able to prolong and extend the distribution of the macromolecule in the whole intestine, even in the colon.

***In vivo* biodistribution of curcumin in the intestines**

The biodistribution of curcumin in the different parts of the intestine, 3 h after administration, was assessed by HPLC quantification (Figure 8).

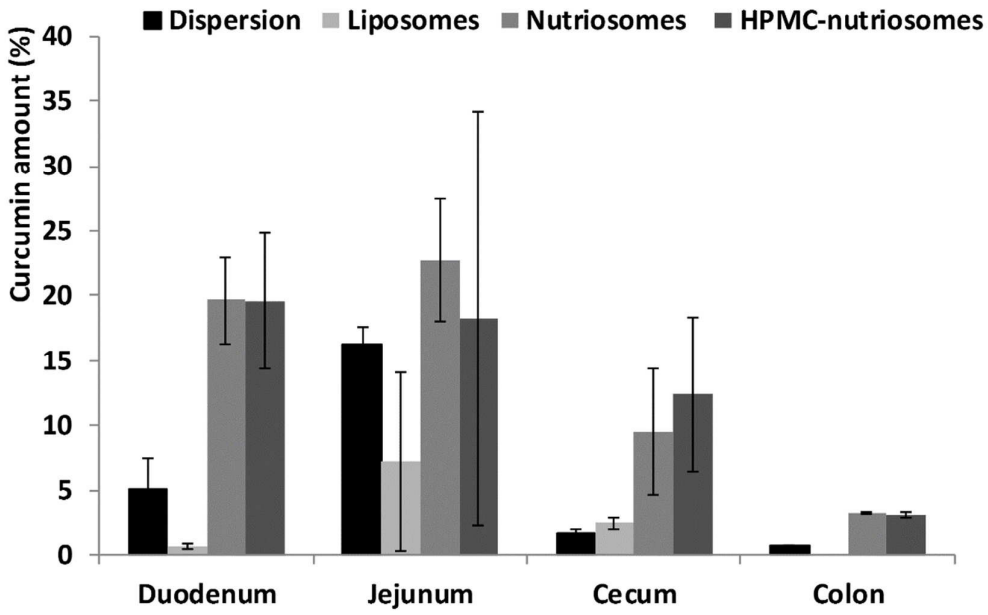

Figure 8. Amount (%) of curcumin found in the different segments of the gastrointestinal tract, 3 h after its administration in aqueous dispersion or in liposomes, nutriosomes and HPMC-nutriosomes. Data are reported as mean values ± standard deviation (error bars).

The dispersion provided a higher accumulation of curcumin in the duodenum (~5%) and jejunum (~16%), and much lower in cecum and colon (~1%). Liposomes allowed a high accumulation in the jejunum (~7%) and cecum (~3%), and less in the other segments (<1%). The accumulation obtained

View Article Online
DOI: 10.1039/C7NR05929A

after administration of nutriosomes and HPMC-nutriosomes was similar in the duodenum and jejunum (~20%), while it was higher in the cecum (~12%) and colon (~3%). In agreement with the biodistribution of the hydrophilic marker, this study confirmed the superior ability of nutriosomes and HPMC-nutriosomes to facilitate the local accumulation of curcumin in the intestines. *In vivo* biodistribution results showed that the amount of curcumin found in liver and kidneys was negligible (data not shown).

Pharmacokinetics of curcumin

The pharmacokinetic studies showed the effect of the nanoincorporation on curcumin plasma concentration. Curcumin levels in blood were determined at 10 different time points up to 8 h after a single dose of dispersion or vesicle formulations administered in rats orally (Figure 9).

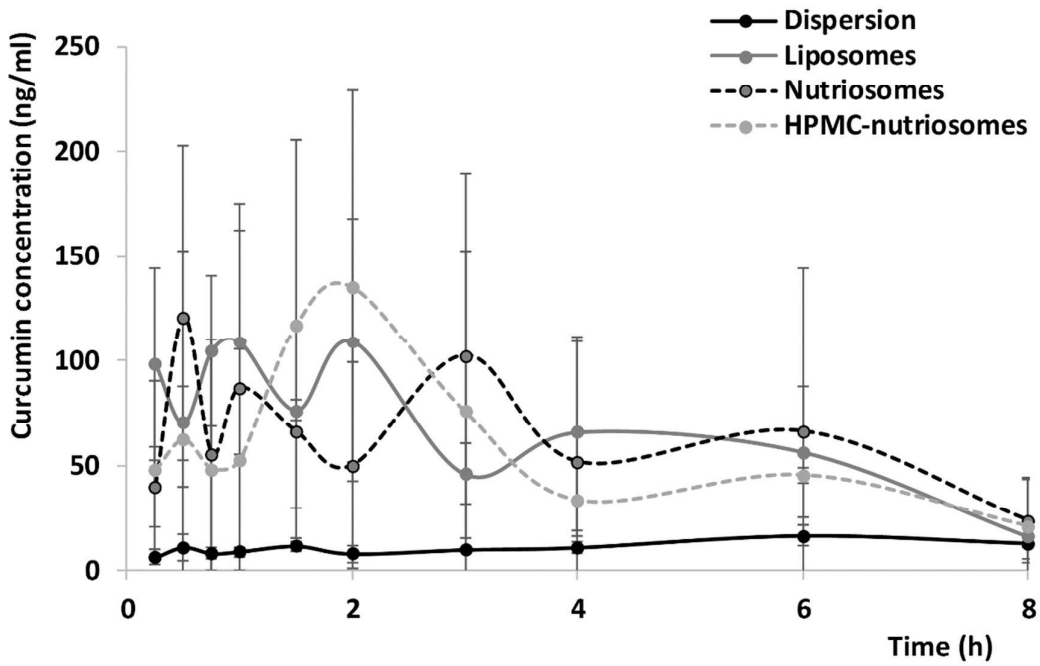

Figure 9. Curcumin plasma concentration over 8 h after a single-dose administration of an aqueous dispersion or liposomes, nutriosomes and HPMC-nutriosomes. Data are reported as mean values ± standard deviation (error bars).

View Article Online
DOI: 10.1039/C7NR05929A

The plasma concentration of curcumin was not detectable when administering 30 mg of the polyphenol in aqueous dispersion, and a double amount (60 mg) was necessary to allow quantification. The plots of plasma concentration *vs*. time displayed a flat and low pharmacokinetic profile for the dispersion, as compared to fluctuating and higher profiles observed for all the vesicle formulations. C_{max}/D and AUC/D were more than 10-, 7.25- and 10.44-fold higher when liposomes, nutriosomes or HPMC-nutriosomes were used, in comparison with the curcumin dispersion. T_{max} results should be interpreted with caution, since the measurement of the curcumin plasma concentration, when the dispersion was administered, did not show a C_{max} as clear and high as that observed when using the vesicle formulations (Figure 9). This demonstrates the carrier capabilities of nutriosomes, which facilitated not only the curcumin local accumulation in the whole intestine, but also the passage of the polyphenol through the intestinal mucosa towards the systemic circulation, providing a maximum concentration 12-15-fold higher (C_{max}/D), and an overall exposure up to 10-fold higher (AUC_{last}/D) than that of the dispersion using half of the dose.

***In vivo* efficacy of curcumin against colitis**

Colitis was induced in rats by intracolonic application of TNBS, and the therapeutic efficacy of curcumin was assessed as a function of the incorporation in the investigated nutriosomes and liposomes. The tissue damage was macroscopically evaluated by visual inspection of the internal and external walls of the colon (Figure 10). The colon of healthy rats was intact and pink-coloured, with a constant width for the entire length. The colon from TNBS rats treated with saline (positive control) showed thickening, ulcerated mucosal lesions, and oedematous inflammation, which caused strong dilatation. Similar features were observed when the curcumin aqueous dispersion was administered. On the contrary, the colon of the TNBS rats treated with the vesicle formulations were very similar to those of healthy controls, in diameter and colour, especially those treated with nutriosomes, while a reduction in length and small necrotic areas were observed in the animals treated with liposomes and HPMC-nutriosomes.

View Article Online
DOI: 10.1039/C7NR05929A

The colonic damage induced by TNBS was associated with an increase in MPO activity in comparison with healthy controls, indicative of neutrophil infiltration in the inflamed tissue.

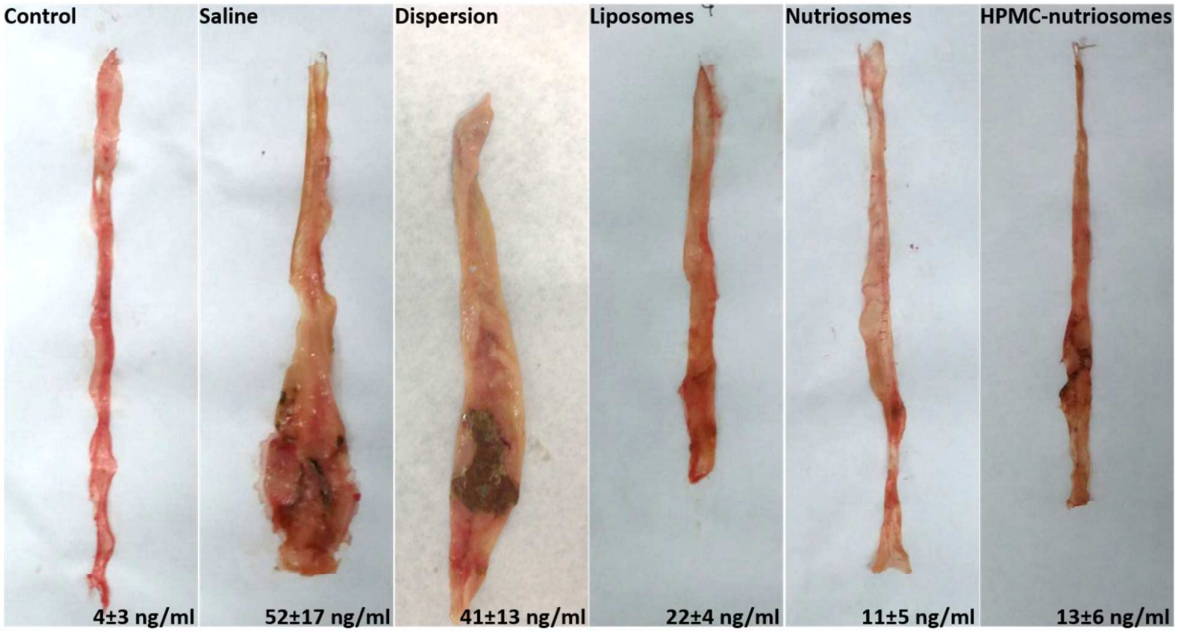

Figure 10. Macroscopic appearance of colon tissue from healthy or colitic rats treated with a curcumin aqueous dispersion or liposomes, nutriosomes and HPMC-nutriosomes. MPO values are reported in ng/ml.

The MPO activity increased significantly in TNBS rats (from 4 to 52 ng/ml; Figure 10), and it was slightly mitigated by the curcumin dispersion. On the other hand, the administration of curcumin loaded vesicles resulted in a marked reduction of MPO activity, especially using nutriosomes and HPMC-nutriosomes (~12 ng/ml; Figure 10), even if the values were not statistically different ($p>0.05$) from that found for liposome-treated animals. The results indicate that liposomes potentiate the ability of curcumin to inhibit MPO, which could not be further extended by nutriosomes and HPMC-nutriosomes, despite the higher bioavailability of the polyphenol they provide.

View Article Online
DOI: 10.1039/C7NR05929A

4. DISCUSSION

Environmental pollution, modern food and beverages contain additives that can cause oxidative stress in human intestine. The cellular antioxidants are not able to neutralize the overproduced reactive oxygen species (ROS), which results in chronic bowel inflammation and systemic oxidative stress, frequently correlated with carcinogenesis [21].

The findings of the present work confirm that the combination of phospholipid, prebiotic dextrin and antioxidant curcumin in a novel phospholipid vesicle formulation, namely nutriosomes, represents a promising approach to prevent and counteract the above physio-pathological conditions. Moreover, nutriosomes were prepared without the use of organic solvents, by means of a one-step, easy and scalable procedure.

Cryo-TEM and SAXS studies displayed that nutriosomes assembled in unilamellar and multilamellar, multicompartment vesicles, stabilized by the presence of Nutriose® in the inter-lamellar and inter-vesicle medium. The presence of curcumin reduced notably the number of multilamellar vesicles. Additionally, HPMC reduced the vesicle lamellarity producing almost unilamellar-only structures, probably due to the polymer adsorption onto the bilayer surface. The soluble dextrin played an important role as a cryo-protector, avoiding vesicle collapse during the lyophilization process: both nutriosomes and HPMC-nutriosomes, when freeze-dried and stored under vacuum up to 180 days, could be easily re-formed by rehydration, basically preserving their size and structure. The high phospholipid concentration (160 mg/ml) used to prepare the vesicles ensured an acceptable resistance of liposomes to high ionic strength and pH changes encountered in the gastrointestinal environment. The additional presence of Nutriose® improved the resistance of nutriosomes, and HPMC further protected the vesicles, presumably thanks to the formation of a polymer layer around the surface of the vesicles. It seems reasonable to presume that the incorporation of curcumin in the vesicles prevented direct contact of the polyphenol with the gastro-intestinal media and its degradation.

View Article Online
DOI: 10.1039/C7NR05929A

When the formulations reach the intestines, intact vesicles could enhance the ability of curcumin to neutralize reactive oxygen species associated to oxidative injury in cells [22–24]. The protective effect against hydrogen peroxide-induced oxidative stress in Caco-2 cells, which were used as intestinal cell model because they grow as monolayer and express several morphological and biochemical characteristic of the small intestine enterocytes [25], was evaluated using curcumin in aqueous dispersion or loaded in vesicles. The highest survival of stressed cells was obtained when nutriosomes and mostly HPMC-nutriosomes were used, while the curcumin dispersion was not able to counteract the oxidative effect of hydrogen peroxide. The results confirmed the great ability of nutriosomes to interact with cells and promote the local antioxidant effect of the polyphenol. Its efficacy was further improved by HPMC-nutriosomes, possibly due to the more extensive cell internalisation (Figure 6). Moreover, other factors could contribute to potentiate the curcumin efficacy using HPMC-nutriosomes, such as increased stability, bioavailability, and release rate, which was slower as compared to liposomes (Figure 5).

Nutriosomes exhibited large affinity and distribution towards the epithelial mucosal surface of the intestine, improving to a large extent the local accumulation of both curcumin and water-soluble, macromolecular phycocyanin, used to simulate the fate of Nutriose®, with respect to a dispersion of the polyphenol and phycocyanin, and liposomes.

Previous pharmacokinetic studies on curcumin reported a low intestinal absorption after oral administration, resulting in poor systemic bioavailability and rapid clearance from the body [26–29]. To overcome these problems, several curcumin nanoformulations have been developed and tested [30,31]. Maiti et al. reported the formation of a curcumin complex with phospholipids capable of enhancing its therapeutic efficacy, which was related to better absorption and bioavailability of the molecule [32]. In this work, curcumin incorporated in liposomes, nutriosomes, and HPMC-nutriosomes showed higher systemic bioavailability (7.44-10.44 fold) in plasma than that provided by the dispersion upon oral administration. Additionally, the vesicles promoted the distribution of curcumin in the intestinal membrane to a greater extent than the free polyphenol in dispersion. Hence, the vesicles

View Article Online
DOI: 10.1039/C7NR05929A

could modify the pharmacokinetics and biodistribution of the incorporated curcumin. A similar enhanced effect was previously found by other authors, and might be attributed to an improved diffusion of particles through the mucus, and a higher interaction with the epithelial walls due to the adhesive properties of nanocarriers [32–34].

In addition, the degree of inflammation and tissue injury caused by TNBS was substantially reduced in rats treated with the vesicle formulations, as demonstrated by the reduction of inflammation biomarkers in comparison with the curcumin dispersion.

5. CONCLUSIONS

In the present study, nutriosomes were successfully developed by combining phospholipids at high concentration, a prebiotic dextrin, an antioxidant polyphenol, and possibly a polymer, by using a simple, organic solvent-free, reproducible method. Nutriosomes were proposed as an oral formulation for the protection of intestine, thanks to the combined activity of Nutriose® and curcumin. Physico-chemical investigations demonstrated that the association of the dextrin and the polyphenol in phospholipid vesicles was crucial for vesicle features and stability. Moreover, the results obtained *in vivo* supported the hypothesis that nutriosomes enhanced the accumulation of both the dextrin and curcumin in the different segments of the intestine. The systemic bioavailability of curcumin was also increased after oral administration of the vesicle formulations. Additionally, chemically-induced colonic damage was reduced by the vesicles, in particular by nutriosomes thanks to the association of the prebiotic dextrin and the antioxidant curcumin.

Overall results suggest that curcumin nutriosomes represent a promising tool for the intestinal treatment of oxidative stress injuries, and they can be proposed for the development of functional foods, dietary supplements, and pharmaceutical preparations thanks to their easy preparation method, biocompatibility and promising performances *in vivo*.

ACKNOWLEDGMENTS

View Article Online
DOI: 10.1039/C7NR05929A

SAXS experiments were performed at the BL11-NCD beamline of the ALBA Synchrotron facility with the collaboration of ALBA staff. The beam-time at ALBA was kindly provided within the approved proposal n. 2013110789. The research leading to these results has received funding from the European Community's Seventh Framework Program (FP7/2007-2013) under the grant agreement n. 312284.

View Article Online
DOI: 10.1039/C7NR05929A

REFERENCES

1 D. Grizard and C. Barthomeuf, *Reprod. Nutr. Dev.*, 1999, **39**, 563–588.

2 J. W. Anderson, B. M. Smith and N. J. Gustafson, *Am. J. Clin. Nutr.*, 1994, **59**, 1242S–1247S.

3 I. I. Ivanov and K. Honda, *Cell Host Microbe*, 2012, **12**, 496–508.

4 L. Guerin-Deremaux, F. Ringard, F. Desailly, D. Wils, W. Timm, Y. Açil, C. Glüer, J. Schrezenmeir, C. Bouteloup-Demange and Y. Rayssiguier, *Nutr. Res. Pract.*, 2010, **4**, 470.

5 W. Pasman, D. Wils, M.-H. Saniez and A. Kardinaal, *Eur. J. Clin. Nutr.*, 2006, **60**, 1024–1034.

6 I. Castangia, A. Nácher, C. Caddeo, V. Merino, O. Díez-Sales, A. Catalán-Latorre, X. Fernàndez-Busquets, A. M. Fadda and M. Manconi, *Acta Biomater.*, 2015, **13**, 216–27.

7 A. R. Martín, I. Villegas, C. La Casa and C. Alarcón De La Lastra, *Biochem. Pharmacol.*, 2004, **67**, 1399–1410.

8 E. O. Farombi, I. A. Adedara, B. O. Ajayi, O. R. Ayepola and E. E. Egbeme, *Basic Clin. Pharmacol. Toxicol.*, 2013, **113**, 49–55.

9 G. Serreli, A. Incani, A. Atzeri, A. Angioni, M. Campus, E. Cauli, R. Zurru and M. Deiana, *J. Food Sci.*, 2017, **82**, 380–385.

10 E. Blanco-García, F. J. Otero-Espinar, J. Blanco-Méndez, J. M. Leiro-Vidal and A. Luzardo-Álvarez, *Int. J. Pharm.*, 2017, **518**, 86–104.

11 J. S. Lee, H. W. Kim, D. Chung and H. G. Lee, *Food Hydrocoll.*, 2009, **23**, 2226–2233.

12 C. Caddeo, R. Pons, C. Carbone, X. Fernàndez-Busquets, M. C. Cardia, A. M. Maccioni, A. M. Fadda and M. Manconi, *Carbohydr. Polym.*, 2017, **157**, 1853–1861.

13 C. Mura, A. Nacher, V. Merino, M. Merino-Sanjuan, C. Carda, A. Ruiz, M. Manconi, G. Loy, A. M. Fadda and O. Diez-Sales, *Int. J. Pharm.*, 2011, **416**, 145–154.

14 I. Castangia, A. Nácher, C. Caddeo, D. Valenti, A. M. Fadda, O. Díez-Sales, A. Ruiz-Saurí and M. Manconi, *Acta Biomater.*, 2014, **10**, 1292–1300.

View Article Online
DOI: 10.1039/C7NR05929A

15 M. Manconi, M. L. Manca, D. Valenti, E. Escribano, H. Hillaireau, A. M. Fadda and E. Fattal, *Int. J. Pharm.*, 2017, **525**, 203–210.

16 W.-C. Hung, F.-Y. Chen, C.-C. Lee, Y. Sun, M.-T. Lee and H. W. Huang, *Biophys. J.*, 2008, **94**, 4331–4338.

17 I. Castangia, M. L. Manca, P. Matricardi, C. Sinico, S. Lampis, X. Fernàndez-Busquets, A. M. Fadda and M. Manconi, *Int. J. Pharm.*, 2013, **456**, 1–9.

18 M. L. Manca, I. Castangia, P. Matricardi, S. Lampis, X. Fernàndez-Busquets, A. M. Fadda and M. Manconi, *Colloids Surf. B. Biointerfaces*, 2014, **117**, 360–367.

19 H. K. Syed, K. Bin Liew, G. O. K. Loh and K. K. Peh, *Food Chem.*, 2015, **170**, 321–326.

20 M. Manconi, J. Pendas, Ledon, N, T. Moreira, C. Sinico, L. Saso and A. M. Fadda, *J. Pharm. Pharmacol.*, 2009, **61**, 423–430.

21 S. Sen and R. Chakraborty, 2011, pp. 1–37.

22 H. H. . Cohly, A. Taylor, M. F. Angel and A. K. Salahudeen, *Free Radic. Biol. Med.*, 1998, **24**, 49–54.

23 X.-C. Zhao, L. Zhang, H.-X. Yu, Z. Sun, X.-F. Lin, C. Tan and R.-R. Lu, *Food Chem.*, 2011, **129**, 387–394.

24 R. K. Maheshwari, A. K. Singh, J. Gaddipati and R. C. Srimal, *Life Sci.*, 2006, **78**, 2081–2087.

25 Y. Sambuy, I. De Angelis, G. Ranaldi, M. L. Scarino, A. Stammati and F. Zucco, *Cell Biol. Toxicol.*, 2005, **21**, 1–26.

26 P. Anand, A. B. . Kunnumakkara, R. A. . Newman and B. B. . Aggarwal, Bioavailability of Curcumin: Problems and Promises, http://pubs.acs.org/doi/pdf/10.1021/mp700113r, (accessed 9 March 2015).

27 M.-H. Pan, T.-M. Huang and J.-K. Lin, *Drug Metab. Dispos.*

28 V. Ravindranath and N. Chandrasekhara, *Toxicology*, 1980, **16**, 259–265.

29 R. A. Sharma, C. R. Ireson, R. D. Verschoyle, K. A. Hill, M. L. Williams, C. Leuratti, M. M.

View Article Online
DOI: 10.1039/C7NR05929A

Manson, L. J. Marnett, W. P. Steward and A. Gescher, *Clin. Cancer Res.*, 2001, **7**, 1452–8.

30 J. Shaikh, D. D. Ankola, V. Beniwal, D. Singh and M. N. V. R. Kumar, *Eur. J. Pharm. Sci.*, 2009, **37**, 223–230.

31 F. Akhtar, M. M. A. Rizvi and S. K. Kar, *Biotechnol. Adv.*, 2012, **30**, 310–320.

32 K. Maiti, K. Mukherjee, A. Gantait, B. P. Saha and P. K. Mukherjee, *Int. J. Pharm.*, 2007, **330**, 155–163.

33 M. Takahashi, S. Uechi, K. Takara, Y. Asikin and K. Wada, *J. Agric. Food Chem*, 2009, **57**, 9141–9146.

34 N. Hussain, *Adv. Drug Deliv. Rev.*, 2001, **50**, 107–142.

View Article Online
DOI: 10.1039/C7NR05929A

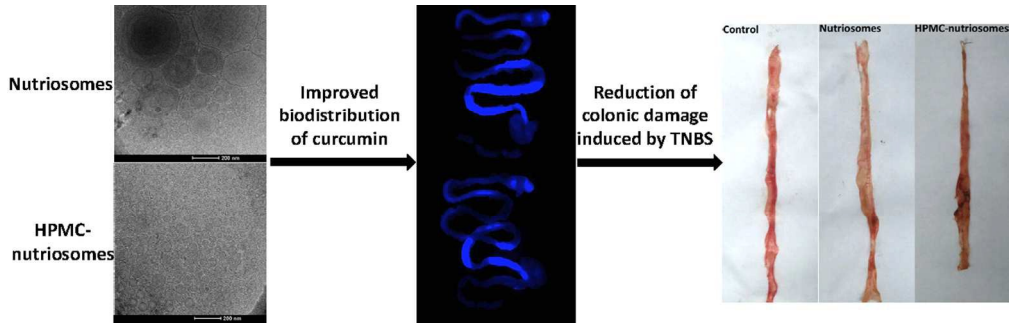

221x70mm (151 x 151 DPI)